

**AN INVESTIGATION OF PHOTONIC BAND
STRUCTURE FOR METALLIC PHOTONIC
CRYSTALS**

by

LOW KHEE LAM

**Thesis submitted in fulfillment of the requirements
for the degree of
Doctor of Philosophy**

MAY 2011

ACKNOWLEDGEMENTS

First and foremost, I would like to express my gratitude to my supervisors Assoc. Prof. Mohd Zubir Mat Jafri and Assoc. Prof. Sohail Aziz Khan for their encouragement, guidance, and endless support in this research project. They have given me continuous motivation and assistance. They will always be role models to me—great advisors, teachers, and researchers. I would like express my sincere gratitude to Prof. Vladimir Kuzmiak for his many valuable suggestions; I am grateful to Dr. Linus Lau from CST for his endless support in CST software. I would like to thank the Ministry of Science, Technology and Innovation (MOSTI) for granting me a scholarship of the National Science Fellowship (NSF). I would like to thank the Ministry of Higher Education (MOHE) for a Fundamental Research Grants Scheme (FRGS, Grant No. 203/PFIZIK/671166 and Grant No. 203/PFIZIK/6711146) and the Institute of Postgraduate Studies of Universiti Sains Malaysia for a Postgraduate Research Grant (PRGS, Grant No. 1001/PFIZIK/841028) to finance the project.

For my family, I am indebted to them too; especially my wife, Kua Wen Chyi, who has been tolerant, patient, and supportive all this while to encourage me to go on. I am thankful to my parents for their sacrifices and support. Without the constant support and encouragement from all of them, it would have been impossible to accomplish this study.

TABLES OF CONTENTS

Acknowledgements	ii
Table of Contents	iii
List of Tables	x
List of Figures	xi
List of Abbreviations	xxi
Abstrak	xxii
Abstract	xxiv
CHAPTER 1 INTRODUCTION	
1.1 Photonic Crystals	1
1.2 History of Photonic Crystals	2
1.3 Numerical Method	5
1.4 Photonic Band Structure (Energy Band)	7
1.5 Left Handed Materials (LHMs) and Effective Plasma Frequency	8
1.6 Materials	13
1.7 Simulation Software	14
1.8 Objectives	15
1.9 Thesis Overview	15
CHAPTER 2 PHOTONIC CRYSTALS THEORY AND METHODOLOGY	
2.1 Introduction	18
2.2 Lattices and Reciprocal Lattices Theory	18
2.3 Bloch's Theorem	20
2.4 Filling Fraction and Brillouin Zone	20
2.4.1 Square Lattice	22
2.4.2 Triangular Lattice	23

2.5 Plane Wave Expansion Method	24
2.5.1 Formula	25
2.6 Field Distribution	29
2.7 Summary	30
CHAPTER 3 INVESTIGATION OF PHOTONIC CRYSTALS BAND STRUCTURE	
3.1 Introduction	31
3.2 Photonic Band Structure of Vacuum Rods in Different Dielectric Materials in Square Lattice Arrangement for H Polarization Mode	31
3.2.1 Vacuum Rods in Silicon Dioxide	31
3.2.2 Vacuum Rods in FR-4	34
3.2.3 Vacuum Rods in Galium Arsenide (GaAs)	34
3.3 Photonic Band Structure of Dielectric Rods in Vacuum in Square Lattice Arrangement for H Polarization Mode	37
3.4 Photonic Band Structure of Vacuum Rods in Different Dielectric Materials in Square Lattice Arrangement for E Polarization Mode	38
3.4.1 Vacuum Rods in Silicon Dioxide	38
3.4.2 Vacuum Rods in FR-4	40
3.4.3 Vacuum Rods in Galium Arsenide (GaAs)	43
3.5 Photonic Band Structure of Dielectric Rods in Vacuum in Square Lattice Arrangement for E Polarization Mode	45
3.5.1 Silicon Dioxide Rods in Vacuum	45
3.5.2 FR-4 Rods in Vacuum	46
3.5.3 Galium Arsenide (GaAs) Rods in Vacuum	48

3.6 Photonic Band Structure of Dielectric Rods in Dielectric Media in Square	
Lattice Arrangement for E and H Polarization Mode	50
3.6.1 Teflon Rods in Gallium Arsenide (GaAs)	50
3.6.2 Teflon Rods in FR-4	52
3.7 Photonic Band Structure of Different Dielectric Material Rods in Vacuum	
in Triangular Lattice Arrangement for H Polarization Mode	52
3.7.1 Silicon dioxide and FR-4 rods in vacuum	52
3.7.2 Gallium Arsenide (GaAs) rods in vacuum	52
3.8 Photonic Band Structure of Vacuum Rods in Different Dielectric Materials	
in Triangular Lattice Arrangement for H Polarization Mode	54
3.8.1 Vacuum Rods in Silicon Dioxide	54
3.8.2 Vacuum Rods in FR-4	54
3.8.3 Vacuum Rods in Gallium Arsenide (GaAs)	56
3.9 Photonic Band Structure of Different Dielectric Material Rods in Vacuum	
in Triangular Lattice Arrangement for E Polarization	57
3.9.1 Silicon Dioxide Rods in Vacuum	57
3.9.2 FR-4 Rods in Vacuum	59
3.9.3 Gallium Arsenide (GaAs) Rods in Vacuum	60
3.10 Photonic Band Structure of Vacuum Rods in Different Dielectric	
Materials in Triangular Lattice for E Polarization	63
3.10.1 Vacuum Rods in Silicon Dioxide	63
3.10.2 Vacuum Rods in FR-4	63
3.10.3 Vacuum Rods in Gallium Arsenide (GaAs)	63
3.11 Dielectric–Dielectric Material Photonic Crystals for Triangular Lattice	
Arrangement	65

3.12 Discussion	67
3.13 Conclusion	71
CHAPTER 4 PHOTONIC CRYSTALS CONTAINING METALLIC COMPONENTS IN E POLARIZATION MODE	
4.1 Introduction	72
4.2 Formula for Metallic Component in Dielectric Slab in E Polarization	73
4.2.1 Dielectric Function	73
4.2.2 Field Equation	75
4.3 Photonic Band Structures for Copper Rods in Different Dielectric Materials in Square Lattice Arrangement	78
4.3.1 Copper Rods in Vacuum	78
4.3.2 Copper Rods in Teflon	79
4.3.3 Copper Rods in FR-4	80
4.3.4 Copper Rods in GaAs	81
4.4 Effective Plasma Frequency of Square Lattices	82
4.5 Photonic Band Structures for Copper Rods in Different Dielectric Materials in Triangular Lattice Arrangement	85
4.5.1 Copper Rods in Vacuum	85
4.5.2 Copper Rods in Teflon	86
4.5.3 Copper Rods in FR-4	87
4.5.4 Copper Rods in GaAs	88
4.6 Effective Plasma Frequency of Triangular Lattices	89
4.7 Discussion	91
4.8 Conclusion	95

CHAPTER 5 PHOTONIC CRYSTALS CONTAINING METALLIC
COMPONENT IN H POLARIZATION MODE

5.1 Introduction	96
5.2 Dielectric Function	96
5.3 Field Equation	97
5.4 Photonic Band Structure of Copper Rods in Different Materials in Square Lattice Arrangement	101
5.4.1 Copper Rods in Vacuum	101
5.4.2 Copper Rods in Teflon	104
5.4.3 Copper Rods in FR-4	106
5.4.4 Copper Rods in GaAs	108
5.5 Photonic Band Structure of Copper Rods in Different Materials in Triangular Lattice Arrangement	109
5.5.1 Copper Rods in Vacuum	109
5.5.2 Copper Rods in Teflon	112
5.5.3 Copper Rods in FR-4	113
5.5.4 Copper Rods in GaAs	114
5.6 Discussion	115
5.7 Conclusion	120

CHAPTER 6 PHOTONIC CRYSTALS OF METALS MEDIUM IN E
POLARIZATION MODE

6.1 Introduction	121
6.2 Formula of Metals Medium with Dielectric Rods	121
6.2.1 Dielectric Function	122
6.2.2 Field Equation	123

6.3 Photonic Band Structure of Different Dielectric Materials of Rods in Copper Media in Square Lattice Arrangement	125
6.3.1 Vacuum Rods in Copper	126
6.3.2 Teflon Rods in Copper	127
6.3.3 FR-4 Rods in Copper	128
6.3.4 GaAs Rods in Copper	129
6.4 Effective Plasma Frequency of Square Lattice	130
6.5 Photonic Band Structure of Different Dielectric Materials of Rods in Copper Media in Triangular Lattice Arrangement	132
6.5.1 Vacuum Rods in Copper	132
6.5.2 Teflon Rods in Copper	133
6.5.3 FR-4 Rods in Copper	134
6.5.4 GaAs Rods in Copper	135
6.6 Effective Plasma Frequency of Square Lattice	136
6.7 Discussion	138
6.8 Conclusion	142
CHAPTER 7 PHOTONIC CRYSTALS OF METALS MEDIUM IN H POLARIZATION MODE	
7.1 Introduction	143
7.2 Dielectric Function	143
7.3 Field Equation	144
7.4 Photonic Band Structure of Different Dielectric Materials of Rods in Copper in Square Lattice Arrangement	147
7.4.1 Vacuum Rods in Copper	147
7.4.2 Teflon Rods in Copper	149

7.4.3 FR-4 Rods in Copper	151
7.4.4 GaAs Rods in Copper	152
7.5 Photonic Band Structure of Different Dielectric Materials of Rods in Copper in Triangular Lattices Arrangement	154
7.5.1 Vacuum Rods in Copper	154
7.5.2 Teflon Rods in Copper	157
7.5.3 FR-4 Rods in Copper	159
7.5.4 GaAs Rods in Copper	160
7.6 Discussion	162
7.7 Conclusion	168
CHAPTER 8 PREMINARY APPLICATION- WAVEGUIDE AND MICROSTRIP	
8.1 Waveguides	169
8.1.1 Result and Discussion	169
8.2 Microstrip	175
8.2.1 Result and Discussion	176
8.3 Conclusion	179
CHAPTER 9 CONCLUSION AND FUTURE STUDY	
9.1 Conclusion	180
9.2 Future Studies	182
9.2.1 Experiment Study	182
9.2.2 Materials	183
REFERENCES	185
LIST OF PUBLICATIONS FROM THESIS	194

List of Tables

		Page
Table 3.1	Band gap at filling fraction $f = 0.2$ and $f = 0.3$ of E polarization.	46
Table 3.2	Band gaps of various filling fractions of photonic crystals with teflon rods in GaAs at E polarization.	51
Table 3.3	Band gap sizes of the second and the third band for photonic crystals with vacuum rods in GaAs in E polarization mode.	64
Table 3.4	Summary of changes of band gap size of suggested materials with filling fraction.	69
Table 4.1	Summary of band gap size changes in the tested materials.	91
Table 4.2	Slope of second lowest band for tested materials in Γ -X direction.	92
Table 4.3	Parameters and root mean square for the effective plasma frequency equation in all filling fractions.	94
Table 5.1	Summary of existence of band gaps in materials studied for E polarization and H polarization (from Chapters 4 and 5).	117
Table 6.1	Summary of band gap sizes changes for various materials.	139
Table 6.2	Slope of second lowest band for materials considered in Γ -X.	140
Table 6.3	Parameters and root mean square for the effective plasma frequency equation in all filling fractions.	141
Table 7.1	Summary of existence of band gaps for materials considered for E and H polarization modes (from chapter 6 and chapter 7).	165

List of Figures

		Page
Figure 1.1	Illustration of 1-D, 2-D, and 3-D photonic crystals (Johnson, 2007).	2
Figure 1.2	Dispersion graph of photonic crystals. Two-dimension triangular lattice with gallium arsenide as background material, embedded with vacuum rods (Sakoda, 2005).	3
Figure 1.3	Illustration of a photonic crystals circuit (Johnson, 2007).	5
Figure 1.4	The effective plasma frequency as the function of rod radius using the expressions of (A) Pendry, 1996; Pendry et al. 1998, (B) Sarychev and Shalaev (2001), (C) Maslovski et al. (2002), and (D) Tretyakov (2004), where the lattice constant is 400 μm with copper rods in vacuum (Brand et al., 2007).	12
Figure 2.1	Irreducible Brillouin zones (red region) for (a) square lattice (b) triangular lattice.	22
Figure 2.2	Photonic crystals of 2 dimensional square lattice a) cross section view b) top view.	24
Figure 2.3	Top view of the 2 dimensional triangular lattice photonic crystals	25
Figure 3.1	Photonic band structure of square lattice with vacuum rods in silicon dioxide ($\epsilon_s = 3.2$) at (a) $f = 0.001$ (b) $f = 0.5$ for H polarization.	33
Figure 3.2	Photonic band structure of square lattice with vacuum rods in FR-4 ($\epsilon_s = 4.9$) at $f = 0.5$ for H polarization.	34
Figure 3.3	H polarization of band structure of square lattice with GaAs ($\epsilon_s = 12.96$) and vacuum rods at $f = 0.5$.	36
Figure 3.4	Changes of band gap between first and second band (Gap 1) against filling fraction for photonic crystals GaAs with vacuum rods for H polarization (square lattice).	36
Figure 3.5	Changes of band gap between second and third band (Gap 2) against filling fraction for photonic crystals GaAs with vacuum rods for H polarization (square lattice).	37
Figure 3.6	Photonic band structure of square lattice with (a) silicon dioxide rods ($\epsilon_s = 3.2$), (b) FR-4 ($\epsilon_s = 4.9$), (c) GaAs	38

($\epsilon_s = 12.96$) in vacuum at $f = 0.5$ for H polarization.

- Figure 3.7 Photonic band structure of square lattice with silicon dioxide ($\epsilon_s = 3.2$) and vacuum rods at (a) $f = 0.001$ (b) $f = 0.5$ for E polarization. 39
- Figure 3.8 Photonic band structure of square lattice with vacuum rods in FR-4 ($\epsilon_s = 4.9$) at (a) $f = 0.5$ (b) $f = 0.7$. For the latter the band gap is centered at $\frac{\omega a}{2\pi c} = 0.3773$ for E polarization. 42
- Figure 3.9 Field Distribution with $\frac{\omega a}{2\pi c} = 0.3773$ for FR-4 and vacuum rods photonic crystals. 42
- Figure 3.10 Band gap size against filling fraction for photonic crystals for vacuum rods in FR-4 in E polarization (square lattice). 43
- Figure 3.11 Photonic band structure of square lattice with vacuum rods in GaAs ($\epsilon_s = 12.96$) at $f = 0.5$ for E polarization. 44
- Figure 3.12 Changes of band gap sizes against filling fraction for photonic crystals with vacuum rods in GaAs for E polarization (square lattice). 44
- Figure 3.13 Photonic band structure of square lattice with silicon dioxide rods ($\epsilon_s = 3.2$) in vacuum at $f = 0.3$ for E polarization. The shaded area is the band gap. 45
- Figure 3.14 Photonic band structure of square lattice with FR-4 rods ($\epsilon_s = 4.9$) in vacuum at $f = 0.1$ for E polarization. Shaded area is the band gap. 47
- Figure 3.15 Changes of band gap size against filling fraction of photonic crystals with FR-4 rods in vacuum for E polarization mode (square lattice). 47
- Figure 3.16 Photonic band structure of square lattice with GaAs rods ($\epsilon_s = 12.96$) in vacuum at $f = 0.2$ for E polarization. Shaded areas are the band gaps. 49
- Figure 3.17 Changes of band gap size against filling fraction of photonic crystals with GaAs rods in vacuum for E polarization mode (a) Gap 1 (b) Gap 2 (square lattice). 50
- Figure 3.18 Photonic band structure of square lattice with teflon rods 51

($\epsilon_0 = 2$) in GaAs ($\epsilon_0 = 12.96$) at $f = 0.9$ for E polarization. Shaded areas are the band gaps.

Figure 3.19	Photonic band structure of triangular lattice with GaAs rods ($\epsilon_0 = 12.96$) in vacuum at $f = 0.5$ for H polarization.	53
Figure 3.20	Variation of band gap size against filling fraction of photonic crystals GaAs rods in vacuum for H polarization (triangular lattice).	53
Figure 3.21	Photonic band structure of triangular lattice with vacuum rods in FR-4 ($\epsilon_0 = 4.9$) at $f = 0.7$ for H polarization.	55
Figure 3.22	Changes of band gap size against filling fraction of photonic crystal vacuum rods in FR-4 for H polarization (triangular lattice).	55
Figure 3.23	Photonic band structure of triangular lattice with vacuum rods in GaAs ($\epsilon_0 = 12.96$) at $f = 0.5$ for H polarization.	56
Figure 3.24	Changes of band gap size against filling fraction of photonic crystals of vacuum rods in GaAs for H polarization (triangular lattice).	57
Figure 3.25	Photonic band structure of triangular lattice with silicon dioxide rods ($\epsilon_0 = 3.2$) in vacuum at $f = 0.5$ for E polarization. Shaded area is band gap.	58
Figure 3.26	Changes of band gap size against filling fraction of photonic crystals silicon dioxide rods in vacuum for E polarization (triangular lattice).	58
Figure 3.27	Photonic band structure of triangular lattice with FR-4 rods ($\epsilon_0 = 4.9$) in vacuum at $f = 0.5$ for E polarization.	59
Figure 3.28	Changes of band gap size against filling fraction of photonic crystals FR-4 rods in vacuum for E polarization (Gap 1).	60
Figure 3.29	Photonic band structure of triangular lattice with GaAs rods ($\epsilon_0 = 12.96$) in vacuum at $f = 0.5$ for E polarization.	61
Figure 3.30	Changes of band gap size against filling fraction of photonic crystals GaAs rods in vacuum for E polarization (a) Gap 1 (b) Gap 2 (triangular lattice).	62
Figure 3.31	Photonic band structure of triangular lattice with vacuum rods in GaAs ($\epsilon_0 = 12.96$) at $f = 0.7$ for E polarization.	64

Figure 3.32	Photonic band structure of triangular lattice with teflon rods ($\epsilon_s = 2$) in GaAs ($\epsilon_s = 12.96$) at $f = 0.5$ for H polarization.	66
Figure 3.33	Changes of band gap size against filling fraction of photonic crystals with teflon rods in GaAs for H polarization (triangular lattice).	66
Figure 4.1	Illustration of the photonic crystals arrangement (square lattice).	74
Figure 4.2	Photonic band structure of photonic crystals with copper rods in vacuum at $f = 0.5$ for E polarization mode. Shaded area is the band gap.	79
Figure 4.3	Photonic band structure of photonic crystals with copper rods in teflon ($\epsilon_s = 2$) at $f = 0.5$ for E polarization mode.	80
Figure 4.4	Photonic band structure of photonic crystals with copper rods in FR-4 ($\epsilon_s = 4.9$) at $f = 0.5$ for E polarization.	81
Figure 4.5	Photonic band structure of photonic crystals with copper rods in GaAs ($\epsilon_s = 12.96$) at $f = 0.5$ for E polarization mode. Shaded area is the band gap.	82
Figure 4.6	Dielectric constant against effective plasma frequency at $f = 0.5$.	84
Figure 4.7	The effective plasma frequency as the function of rod radius using the expressions of A) Pendry, 1996; Pendry et al. 1998, (B) Sarychev and Shalaev (2001), (C) Maslovski et al. (2002), and (D) Tretyakov (2004), where the lattice constant is $1 \mu\text{m}$ with copper rods in vacuum.	84
Figure 4.8	Effective plasma frequency against radius of rods for various dielectric backgrounds with copper rods.	85
Figure 4.9	Photonic band structure of photonic crystals with copper rods in vacuum at $f = 0.5$ for E polarization.	86
Figure 4.10	Photonic band structure of photonic crystals with copper rods in teflon ($\epsilon_s = 2$) at $f = 0.5$ for E polarization.	87
Figure 4.11	Photonic band structure of photonic crystals with copper rods in FR-4 ($\epsilon_s = 4.9$) at $f = 0.5$ for E polarization. Shaded area is the band gap.	88

Figure 4.12	Photonic band structures of photonic crystals with copper rods in GaAs ($\epsilon_s = 12.96$) at $f = 0.5$ for E polarization. Shaded areas are the band gaps.	89
Figure 4.13	Effective plasma frequency against dielectric constant of photonic crystal copper rods in dielectric media at $f = 0.5$.	90
Figure 4.14	Effective plasma frequency against radius of rods for various dielectric containing copper rods in E polarization mode.	90
Figure 5.1	Photonic band structure of square lattice with copper rods in vacuum at $f = 0.001$ for H polarization.	102
Figure 5.2	Photonic band structure of photonic crystals with copper rods in vacuum at $f = 0.5$ for H polarization. (a) Ranging from $\frac{\omega a}{2\pi c} = 0$ to $\frac{\omega a}{2\pi c} = 1.6$ (b) Ranging from $\frac{\omega a}{2\pi c} = 0.5$ to $\frac{\omega a}{2\pi c} = 1.2$.	103
Figure 5.3	Photonic band structure of photonic crystals with copper rods in teflon ($\epsilon_s = 2$) at $f = 0.5$ for H polarization. (a) Ranging from $\frac{\omega a}{2\pi c} = 0$ to $\frac{\omega a}{2\pi c} = 1.6$ (b) Ranging from $\frac{\omega a}{2\pi c} = 0.5$ to $\frac{\omega a}{2\pi c} = 1.2$.	105
Figure 5.4	Photonic band structure of photonic crystals with copper rods in FR-4 ($\epsilon_s = 4.9$) at $f = 0.5$ for H polarization. (a) Ranging from $\frac{\omega a}{2\pi c} = 0$ to $\frac{\omega a}{2\pi c} = 1.2$ (b) Ranging from $\frac{\omega a}{2\pi c} = 0.5$ to $\frac{\omega a}{2\pi c} = 1.2$ (Shaded area is band gap for all directions).	107
Figure 5.5	Photonic band structure of photonic crystals with copper rods in GaAs ($\epsilon_s = 12.96$) at $f = 0.5$ for H polarization. (a) Ranging from $\frac{\omega a}{2\pi c} = 0$ to $\frac{\omega a}{2\pi c} = 1.2$ (b) Ranging from $\frac{\omega a}{2\pi c} = 0.6$ to $\frac{\omega a}{2\pi c} = 1.0$	109
Figure 5.6	Photonic band structure of photonic crystals with copper rods in vacuum at (a) $f = 0.001$ (b) $f = 0.5$ for H	111

polarization.

- Figure 5.7 Band gaps of photonic crystals with copper rods in vacuum 111
at $f = 0.001$ in H polarization from $\frac{\omega a}{2\pi c} = 0.8$ to
 $\frac{\omega a}{2\pi c} = 1.2$.
- Figure 5.8 Photonic band structure of photonic crystals with copper 113
rods in teflon ($\epsilon_s = 2$) at (a) $f = 0.5$ (b) ranging from
range $\frac{\omega a}{2\pi c} = 0.8$ to $\frac{\omega a}{2\pi c} = 1.2$ for H polarization.
- Figure 5.9 Photonic band structure of photonic crystals with copper 114
rods in FR-4 ($\epsilon_s = 4.9$) for H polarization. The shaded area
is the band gap.
- Figure 5.10 Photonic band structure of photonic crystals with copper 115
rods in GaAs ($\epsilon_s = 12.96$) at $f = 0.5$ for H polarization.
Shaded area is the band gap.
- Figure 5.11 Photonic band structure for copper rods in vacuum for E 118
and H polarization modes in square lattice.
- Figure 5.12 Absence of photonic band gap for copper rods in GaAs for 118
E and H polarization modes in square lattice.
- Figure 5.13 Photonic band structure for copper rods in vacuum for E 119
and H polarization modes in triangular lattice.
- Figure 5.14 Absence of photonic band gap for copper rods in GaAs for 119
E and H polarization modes in triangular lattice.
- Figure 6.1 Illustration of the metallic photonic crystal arrangement 122
(square lattice).
- Figure 6.2 Photonic band structure for vacuum rods in copper slab at 126
 $f = 0.001$ for E polarization mode.
- Figure 6.3 Photonic band structure for photonic crystals of vacuum 127
rods in copper slab at $f = 0.5$ for E polarization. Shaded
area is the band gap.
- Figure 6.4 Photonic band structure for photonic crystals of teflon 128
($\epsilon_s = 2$) rods in copper slab at $f = 0.5$ for E polarization.
Shaded area is the band gap.

Figure 6.5	Photonic band structure for photonic crystals of FR-4 rods ($\epsilon_r = 4.9$) in copper slab at $f = 0.5$ for E polarization. Shaded area is the band gap.	129
Figure 6.6	Photonic band structure for photonic crystals of GaAs rods ($\epsilon_r = 12.96$) in copper slab at $f = 0.5$ for E polarization. Shaded area is the band gap.	130
Figure 6.7	Effective plasma frequency against dielectric constant of photonic crystals with copper rods at $f = 0.5$.	131
Figure 6.8	Effective plasma frequency against radius of dielectric rods for copper slab.	131
Figure 6.9	Photonic band structure for photonic crystals of vacuum rods in copper slab at (a) $f = 0.001$. (b) $f = 0.5$ for E polarization. Shaded area is the band gap.	133
Figure 6.10	Photonic band structure for photonic crystals of teflon rods ($\epsilon_r = 2$) in copper slab at $f = 0.5$ for E polarization. Shaded area is the band gap.	134
Figure 6.11	Photonic band structure for photonic crystals of FR-4 rods ($\epsilon_r = 4.9$) in copper slab at $f = 0.5$ for E polarization.	135
Figure 6.12	Photonic band structure for photonic crystals of GaAs rods ($\epsilon_r = 12.96$) in copper slab at $f = 0.5$ for E polarization.	136
Figure 6.13	Effective plasma frequency against various dielectric constant of rods at $f = 0.5$.	137
Figure 6.14	Effective plasma frequency against radius of rods for various materials.	138
Figure 7.1	Photonic band structure for photonic crystals of vacuum rods in copper slab at (a) $f = 0.001$ (b) $f = 0.5$ for H polarization.	148
Figure 7.2	Photonic band structure for photonic crystals of vacuum rods in copper slab at $f = 0.5$ for H polarization from 0.6 until 1.2. Shaded area is the band gap.	149
Figure 7.3	Photonic band structure for photonic crystals of teflon rods ($\epsilon_r = 2$) in copper slab at $f = 0.5$ for H polarization.	150
Figure 7.4	Photonic band structure for photonic crystals of teflon rods	150

($\epsilon_s = 2$) in copper slab from $\frac{\omega a}{2\pi c} = 0.6$ until $\frac{\omega a}{2\pi c} = 1.2$ at $f = 0.5$ for H polarization. (Square lattice) Shaded areas are the band gap.

- Figure 7.5 Photonic band structure for photonic crystals of FR-4 rods ($\epsilon_s = 4.9$) in copper slab at $f = 0.5$ for H polarization. 151
- Figure 7.6 Photonic band structure for photonic crystals of FR-4 rods ($\epsilon_s = 4.9$) in copper slab at $f = 0.5$ for H polarization from $\frac{\omega a}{2\pi c} = 0.6$ until $\frac{\omega a}{2\pi c} = 1.2$. Shaded areas are the band gap. 152
- Figure 7.7 Photonic band structure for photonic crystals of GaAs rods ($\epsilon_s = 12.96$) in a copper slab at $f = 0.5$ for H polarization (square lattice). 153
- Figure 7.8 Photonic band structure for photonic crystals of GaAs rods ($\epsilon_s = 12.96$) in copper slab at $f = 0.5$ for H polarization from $\frac{\omega a}{2\pi c} = 0.6$ until $\frac{\omega a}{2\pi c} = 1.2$. 153
- Figure 7.9 Photonic band structure for photonic crystals of vacuum rods in copper slab at (a) $f = 0.001$ (b) $f = 0.5$ for H polarization. 155
- Figure 7.10 Photonic band structure for photonic crystals of vacuum rods in copper slab at $f = 0.5$ for H polarization from (a) $\frac{\omega a}{2\pi c} = 0.8$ until $\frac{\omega a}{2\pi c} = 1.2$ (b) $\frac{\omega a}{2\pi c} = 0$ until $\frac{\omega a}{2\pi c} = 0.5$. 156
- Figure 7.11 Photonic band structure for photonic crystals of teflon rods ($\epsilon_s = 2$) in copper slab at $f = 0.5$ for H polarization. 158
- Figure 7.12 Photonic band structure for photonic crystals of teflon rods ($\epsilon_s = 2$) in copper slab from $\frac{\omega a}{2\pi c} = 0.8$ until $\frac{\omega a}{2\pi c} = 1.2$ at $f = 0.5$ for H polarization. Shaded areas are the band gaps. 158
- Figure 7.13 Photonic band structure for photonic crystals of FR-4 rods ($\epsilon_s = 4.9$) in copper slab at $f = 0.5$ for H polarization. 159
- Figure 7.14 Photonic band structures for photonic crystals of FR-4 rods 160

($\epsilon_0 = 4.9$) in copper slab from $\frac{\omega a}{2\pi c} = 0.8$ to $\frac{\omega a}{2\pi c} = 1.2$ at $f = 0.5$ for H polarization. Shaded areas are the band gaps.

Figure 7.15	Photonic band structure for photonic crystals of GaAs rods ($\epsilon_0 = 12.96$) in copper slab at $f = 0.5$ for H polarization.	161
Figure 7.16	Photonic band structures for photonic crystals of GaAs rods ($\epsilon_0 = 12.96$) in copper slab at $f = 0.5$ for H polarization from $\frac{\omega a}{2\pi c} = 0.8$ to $\frac{\omega a}{2\pi c} = 1.2$. Shaded areas are the band gaps.	162
Figure 7.17	Photonic band structure of GaAs rods with filling fraction $f = 0.5$ in copper media in H polarization. Magnetic field distribution at frequencies (b) 1499 THz, (c) 743 THz, (d) 176 THz.	164
Figure 7.18	Photonic band structure for vacuum rods in copper for E and H polarization at $f = 0.5$ in square lattice.	166
Figure 7.19	Photonic band structure for GaAs rods in metal in E and H polarization mode $f = 0.5$ in square lattice.	166
Figure 7.20	Photonic band structure for vacuum rods in copper for E and H polarization at $f = 0.5$ in triangular lattice.	167
Figure 7.21	Photonic band structure for GaAs rods in metal in E and H polarization mode $f = 0.5$ in triangular lattice.	167
Figure 8.1	3D view of waveguide in CST MWS	169
Figure 8.2	Reflection coefficients (S_{11}) of waveguide from 0 until 0.1THz.	170
Figure 8.3	Photonic band structure of ordinary square lattice structure with vacuum rods in FR-4 ($\epsilon_0 = 4.9$).	171
Figure 8.4	Photonic band structure from Γ to X.	172
Figure 8.5	The designed waveguide.	173
Figure 8.6	Field distribution at frequency $f = 0.05$ THz.	174
Figure 8.7	Field distribution at frequency $f = 0.50$ THz.	174

Figure 8.8	Field distribution at $f= 0.94$ THz.	175
Figure 8.9	Band structure of photonic crystals with copper rods in FR-4 ($\epsilon_r = 4.9$) for radius = 0.17 mm and lattice constant = 0.93 mm.	176
Figure 8.10	Photonic band structure for Γ -X.	177
Figure 8.11	3D view of the photonic crystals base with copper rods in FR-4	177
Figure 8.12	3D view of the microstrip with photonic crystals base	178
Figure 8.13	Normalized transmission coefficients of the microstrip	179

List of Abbreviation

2D	= 2-dimension
3D	= 3-dimension
CST MWS	= CST Microwave Studio Packages
E Polarization	= Electric Polarization
FDFD	= Finite Difference Frequency Domain
FDTD	=Finite Difference Time Domain
FEM	= Finte Element Method
FR-4	= Flame Resistant 4
GaAs	= Gallium Arsenide
H Polarization	= Magnetic Polarization
LHM	= Left Handed Material
MEEP	= MIT Electromagnetic Equation Propagation
PCs	= Photonic Crystals
PTFE	= Polytetrafluoroethylene
SiO ₂	= Silicon Dioxide

KAJIAN STRUKTUR JALUR FOTONIK UNTUK HABLUR FOTONIK LOGAM

ABSTRAK

Hablur fotonik ialah sejenis struktur buatan yang berkala. Keunikan sifatnya merupakan satu daripada tajuk yang paling banyak dikaji sejak 20 tahun lalu. Para penyelidik percaya bahawa struktur ini boleh mengatasi halangan yang dihadapi sekarang dalam bidang penyelidikan berkaitan nano-optik. Dalam tesis ini, sifat hablur fotonik diselidik. Satu daripada parameter paling penting yang mempamerkan sifat atau ciri-ciri hablur fotonik adalah struktur jalur fotoniknya.

Dalam tesis ini, suatu persamaan gelombang satah (plane wave equation, PWE) digunakan untuk mengira struktur jalur fotonik. Vakum, teflon, silikon dioksida, FR-4 dan galium arsenida digunakan untuk mencampur, memadan serta mengkaji struktur jalur fotonik. Keputusan yang diperolehi menjelaskan beberapa kejanggalan sifat hablur fotonik yang terdapat dalam kajian literatur. Dalam kajian literatur, jurang jalur cenderung wujud pada kontras dielektrik yang tinggi, sebagaimana yang diramal oleh John D. Joannopoulos dan para pekerjaannya, tetapi tidak ditemui dalam kajian ini.

Malangnya, kaedah berangka PWE terhad kepada bahan dielektrik bebas frekuensi. Oleh itu, suatu persamaan baru untuk bahan dielektrik yang mengandungi komponen logam (bahan bersandar frekuensi) diterbitkan. Persamaan ini lebih umum berbanding dengan kajian penyelidik terdahulu. Struktur jalur fotonik vakum, teflon, FR-4 dan galium arsenida yang mengandungi rod kuprum dilakar bagi pengutuban E dan H. Rod kuprum dalam teflon bukan merupakan hablur fotonik dalam kedua-dua susunan kekisi segi empat sama dan segi tiga bagi pengutuban E. Sebaliknya, semua bahan boleh berfungsi sebagai hablur fotonik bagi mod pengutuban H dalam kedua-dua susunan kekisi termasuk teflon. Dalam susunan zon Brillouin, arah Γ -X

menunjukkan kesan kejanggalan halaju kumpulan yang ditemui pada jalur terendah ketiga untuk semua bahan bagi pengutuban H. Sifat metabahan tangan-kiri (left-handed metamaterials, LHM) ditemui untuk semua bahan dalam semua susunan kekisi bagi pengutuban E. Satu model analitik baru diterbitkan untuk frekuensi plasma berkesan pengutuban E daripada data simulasi dengan menggunakan analisis statistik.

Berdasarkan pengiraan terbaru ini, kaedah PWE digunakan untuk mengira struktur jalur fotonik yang mengandungi rod dielektrik dalam medium logam (bahan bersandar frekuensi). Oleh itu, suatu persamaan baru diterbitkan. Persamaan ini digunakan untuk melakar struktur jalur fotonik untuk medium kuprum yang mengandungi rod vakum, teflon, FR-4 dan galium arsenida bagi pengutuban E dan H. Rod FR-4 dalam kuprum bagi pengutuban E dalam susunan kekisi segi empat sama dan segi tiga pula tidak berfungsi sebagai hablur fotonik. Selain itu, semua bahan lain boleh berfungsi sebagai hablur fotonik bagi pengutuban E dan H dalam susunan kekisi segi empat sama dan segi tiga. Bahan yang digunakan dalam kajian ini tidak memberi kesan terhadap jurang jalur kerana jurang jalur yang sama muncul pada julat yang sama bagi frekuensi normal dalam mod pengutuban H. Serakan negatif dan frekuensi plasma berkesan yang rendah dikesan bagi rod vakum dan rod teflon dalam kuprum bagi mod pengutuban E, yang merupakan sifat LHM. Kejanggalan halaju kumpulan dan kesan plasmon permukaan dikesan untuk semua bahan dalam mod pengutuban H. Akhir sekali, panduan gelombang dan mikrostrip digunakan untuk aplikasi hablur fotonik.

AN INVESTIGATION OF PHOTONIC BAND STRUCTURE FOR METALLIC PHOTONIC CRYSTALS

ABSTRACT

Photonic crystals are artificial periodic structures. Their unique properties are one of the most extensively studied topics in the past 20 years. Researchers believe that this structure can overcome the challenge that we are facing nowadays in the nano-optics related research field. In this thesis, the nature of photonic crystals has been investigated. One of the most important parameters that exhibits the characteristic or properties of photonic crystals is the photonic band structure.

In this thesis, a plane wave equation (PWE) has been used to calculate the photonic band structure of photonic crystals. Vacuum, teflon, silicon dioxide, FR-4, and gallium arsenide are used to mix, match, and study the photonic crystal photonic band structure. Our results clarify the discrepancies of photonic crystals property in the literature. In the literature, the band gap tends to appear at high dielectric contrast of photonic crystals, which was predicted by John D. Joannopoulos and coworkers, but was not found in this investigation.

Unfortunately, the PWE numerical method is limited to frequency-independent dielectric materials. Therefore a new equation for the dielectric materials containing metallic components (frequency-dependent materials) has been derived. This equation is much more general compared to the previous studies by other researchers. The photonic band structures of vacuum, teflon, FR-4, and gallium arsenide containing copper rods are plotted for E and H polarization. Copper rods in teflon are not photonic crystals in both square and triangular lattice arrangements for the E polarization. But all the materials can work as photonic crystals for the H polarization mode in both square and triangular lattice arrangements including teflon.

In Brillouin zone arrangements, the direction of Γ -X showed the group velocity anomaly effect found at the third lowest band for all the materials in H polarization. Properties of left-handed metamaterials are found for all the materials in all lattice arrangements in the E polarization. A new analytical model is derived for the effective plasma frequency of E polarization from the simulation data using statistical analysis.

By utilizing this new calculation, the plane wave expansion method is used to calculate the photonic band structure of photonic crystals containing dielectric rods in metallic media (frequency-dependent materials). Thus a new equation is derived. This equation is utilized to plot the photonic band structures of copper media containing vacuum, teflon, FR-4, and gallium arsenide rods for E and H polarization. FR-4 rods in copper for E polarization in square and triangular lattice arrangements cannot is not functioning photonic crystals. Other than that, all other materials are functioning as photonic crystals for E and H polarizations in square and triangular lattice arrangements. The materials used in this research do not affect the band gap because the same band gap appears at the same range of the normalized frequency in H polarization mode. A negative refraction and low effective plasma frequency are detected for vacuum rods and teflon rods in copper for E polarization mode, which are the properties of left-handed metamaterials. The group velocity anomaly and the surface plasmons effect are detected for all the materials in H polarization mode. Finally, waveguides and microstrips are used for the application of photonic crystals.

Chapter 1

Introduction

1.1 Photonic Crystals

Photonic crystals (PCs) are artificial periodic dielectric structures. All the dimensions of PCs can be tailored according to the need of scientists. Figure 1.1 shows the basic arrangements of PCs. In 1888, the one-dimensional periodic structure was studied by Lord Rayleigh (1888), who showed that such a system has a one-dimensional photonic band structure. It was only in 1987 that the concept of PCs was developed by Yablonovitch (1987) and Sajeev (1987). They proposed PCs in two dimensions and three dimensions as shown in Figure 1.1. Then, the theory of a periodic structure was used to build the fundamental theory for photonic crystals. Just as the periodicity of solid state crystals determines the energy band structure, the structuring of PCs at wavelength scales has turned out to be viable approach to the control of the photons.

In PCs, there is one unique property, which is the band gap. The band gap is a range of frequencies for which light is forbidden to propagate inside the crystals. There are two kinds of band gap: a partial band gap and a complete band gap. A partial band gap occurs in only one of the polarization modes, whereas a complete band gap occurs at the same place in both polarization modes. A crystal with a complete gap can serve as ideal mirror; on the other hand a partial band gap allows light propagation only along certain directions. The existence of band gaps in photonic crystals was described by a fundamental rule from Joannopoulos et al. (1997), who stated that a band gap appears in high dielectric contrast.

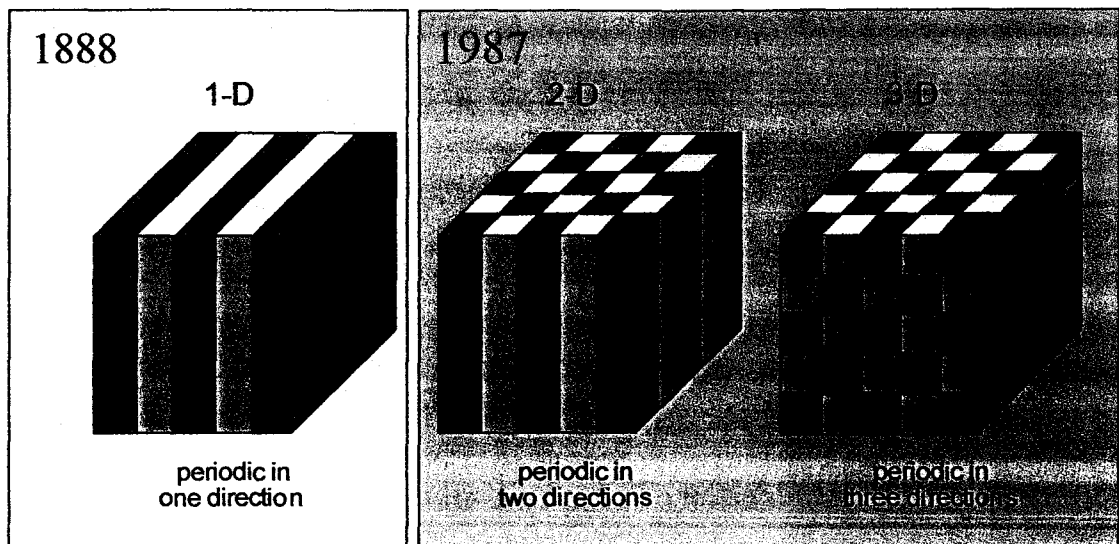


Figure 1.1: Illustration of 1-D, 2-D, and 3-D photonic crystals (Johnson, 2007).

1.2 History of Photonic Crystals

Photonic crystals have been studied rigorously in this decade. The study was first led by Yablonovitch (1987) and Sajeev (1987) who found that the periodic dielectric can control the flow of light. This discovery led to the advent of photonic crystals in physics. This is the beginning of photonic crystal research in the scientific area. It has become one of the most leading fields of research in the world, in which scientists try to understand the basic characteristic of the photonic crystals. They used the fundamental physics of the solid state to study it. The Bloch theorem, reciprocal lattice, and Brillouin zones were adapted from the original solid state physics understanding.

In analogy with the electronic band gaps of semiconductors, band structure graphs of periodic energy are used to describe the fundamental properties of photonic crystals. A periodic dielectric function may result in the formation of photonic band structures. An example of omnidirectional photonic band structures is shown in Figure 1.2 for the E polarization mode. It is a gallium arsenide slab with an array of

holes in vacuum which created a vacuum rods. The shaded grey area is the stop band of the designed photonic crystals. In this area, waves are forbidden.

The extensive development of the solid state has opened up semiconductor technology. It built a strong base for manipulating the current development in the semiconductors. Although scientists have a good understanding of the propagation of electrons in solids, they have yet to manipulate light waves in solids. This breakthrough will open up a new era of information technology.

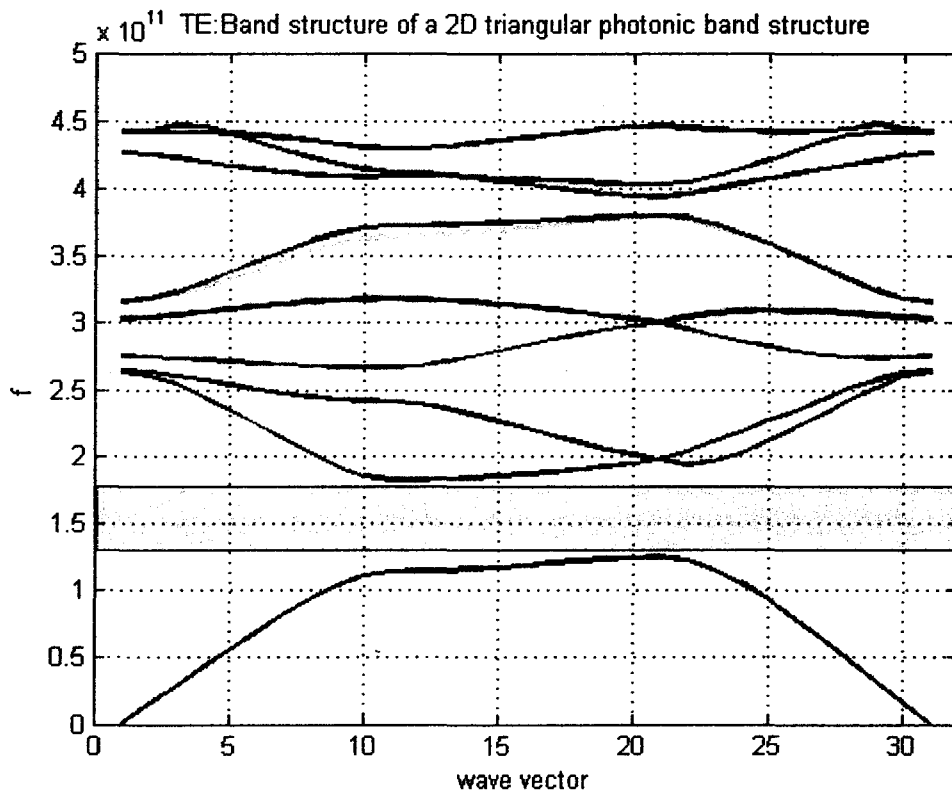


Figure 1.2: Dispersion graph of photonic crystals. Two-dimension triangular lattice with gallium arsenide as background material, embedded with vacuum rods in E polarization mode (Sakoda, 2005).

Photonic band structures are used to determine the working frequency, structure, dimensions, and losses of photonic crystals. This can lead to applications in

antennas, filters, and waveguides. The reflection, localization, refraction, and transmission properties of PCs can be designed. Each of these properties can be used to create unique devices with lower losses. For example, using the localization characteristic of PCs, we can design a waveguide (Lin, 1998; Mekis et al., 1996; Simpson et al., 2006; Tse et al., 2004; Zhao and Grischkowsky, 2007; Ozbay et al., 2003); using the band gap characteristic, we can design a reflecting mirror (Yablonovitch, 1987; Lodahl et al., 2004); using the refraction characteristic, we can design devices utilizing the super prism phenomena (Notomi, 2000) and negative refraction (Luo et al., 2002). Due to these unique characteristics of photonic crystals, scientists have thought of using photonic crystal arrangements for photonic circuits. Photonic crystals are used to control the flow of photons in the photonic circuits as shown in Figure 1.3. This illustration is by Johnson (2007) from MIT, which he believes demonstrates the future of photonic circuits. Each of its components is made from photonic crystals. Beside that, photonic crystals also can be used to confine the flow of microwaves. So, photonic crystals are important in the development of micronanophotonics devices.

The basic characteristics of photonic crystals have led to their replacing of the conventional design of electronic devices. There are a few examples such as antennas (Poilasne et al., 1999; Chiau et al., 2005; Sharma et al., 2008; Brown and Parker, 1993), fiber optics (Knight et al., 1998; Guenneu et al., 2003; Granpayeh, 2009), lasers (Painter et al., 1999), microstrips (Lopotegi et al., 2002; Shahparnia and Ramahi, 2004; Radisic et al., 1998; Parui and Das, 2004; Falcone et al., 2002), filters (Karim et al., 2005), photonic circuits (McGurn, 2000), superconductors (Mao et al., 1996), solar cells (Chutinan et al., 2009), perfect lenses (Pendry, 2000), horns (Weily et al., 2003), waveguides (Pile et al., 2005; Dai and Jiang, 2009; Zhao and

Grischkowsky, 2007), and biomedical and chemical sensors (Kurt and Citrin, 2005; Scherer and Qiu, 2003). Scientists also are beginning to use metallic photonic crystals to study the effect of surface plasmon polaritons (Feng et al., 2008; Hosseini et al., 2008; Crist et al., 2003; Ortuno et al., 2009; Barnes, 1999). Recently, scientists also found out that we can tailor the plasma frequency of metallic as desired with promising results (Xiaochuang et al., 2005; Brand et al., 2007; Qi and Yang, 2009). PCs made from plasma materials also have been studied by several scientists (Sakai et al., 2007; Sakaguchi et al., 2007; Qi and Yang, 2009). These show that the photonic band structure is very important in designing and characterizing all the devices mentioned above.

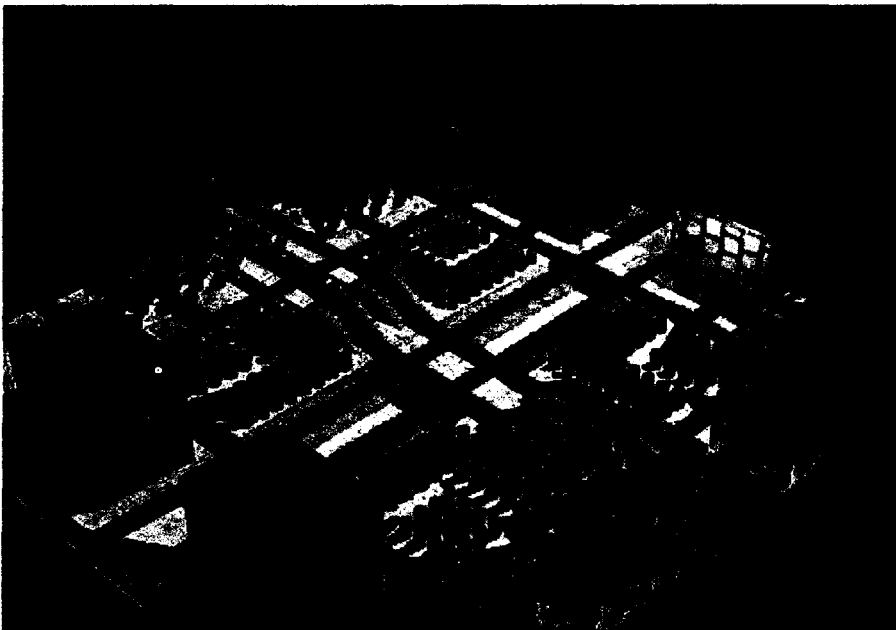


Figure 1.3: Illustration of a photonic crystals circuit (Johnson, 2007).

1.3 Numerical Methods

There are different methods for finding the photonic band structure. (1) The plane wave expansion (PWE) method (Guo and Albin, 2003; Glushko, 2006; Zoli et al.,

2003; Shi et al., 2005; Kuzmiak and Maradudin, 1997; Kuzmiak et al., 1994; Plihal and Maradudin, 1991; Hussein, 2009; Toader and John, 2004), (2) finite differences time domain (FDTD) (Sakoda et al., 2001; Ito and Sakoda, 2001; Li et al., 2005), and (3) super cell and finite differences frequency domain (FDFD) (Xu et al., 2003) have been tried by researchers. The materials of photonic crystals include frequency-independent materials and frequency-dependent materials. It is a very easy approach to calculate the photonic band structure when using the frequency-independent materials. The new challenge is to analyze frequency-dependent materials in photonic crystals. This is because the calculation has to be modified to meet the requirement. Kuzmiak et al. (1994) modified the plane wave expansion method to study the band structure of photonic crystals containing metallic components. Later, they expanded the study using the plane wave expansion to study the field distribution of that structure (Kuzmiak and Maradudin, 1998). Sakoda and coworkers (Sakoda et al., 2001; Ito and Sakoda, 2001) modified the FDTD method to calculate the same structure as Kuzmiak. Moreno et al. (2002) used the multipoint method to calculate the band structure of metallic components. Ustyantsev et al. (2006) showed that the PWE method agreed very well with the FDTD method. But all the calculations are limited to waves in air. No calculations or examples involving materials other than air have been found in the literature.

In the literature, there are no photonic band structure calculations involving photonic crystals in metallic media (frequency-dependent materials). The calculation is very important because several optical properties are predicted to be found, such as negative refraction, effective plasma frequency, group velocity anomaly, and surface plasmons, which are very important for optical devices. So, the photonic band

structure will present a clear picture of all the optical properties of these types of photonic crystals in all directions.

The plane wave expansion method (PWE) was chosen for this thesis work because this method consumes less computational time to compute the band energy graph for all directions. Therefore, the efficiency is increased. Another reason the PWE method was chosen is that the lattice that we are considering has a symmetric structure which produces the best result when using the PWE method. Even though there is no noticeable difference between PWE and FDTD when calculating for the frequency-dependent materials, the advantage is that we don't encounter the converging problem. The converging problem arises from the numerical dispersion that is commonly encountered by FDTD for a frequency-dependent material (Juntunen and Tsiboukis, 2000). The only solution is to increase the resolution of the calculation, which will increase the time as well. In order to calculate the photonic band structures of metallic photonic crystals using the PWE method, the dielectric function of ordinary PWE has to be modified because the dielectric function of frequency-dependent materials must be included in order to find the energy band. So, the main purpose of this research is to generalize a calculation method of photonic crystals for frequency-dependent materials that is able to include all the available solid materials.

1.4 Photonic Band Structure (Energy Band)

In a periodic system, ψ_k are the Bloch waves. The wave vector k is limited in first Brillouin zone. In order to understand wave propagation in a periodic system, all the Bloch waves in the first Brillouin zone are needed. The Bloch waves create a number of eigenvalues, each with a fixed wave vector. Those eigenvalues have angular

frequency ω . When the Bloch waves vary in the Brillouin zones, the eigenvalues also vary accordingly.

Band gaps are the most unique characteristic of photonic crystals. Multiple scattering occurs when a wave propagates through a periodic medium. This leads to the creation of constructive waves and destructive waves in the medium. As a result, there are constructive and destructive areas formed in the medium. Wave cannot propagate in destructive areas, therefore no energy can be transferred there. A band gap occurs in a certain frequency range where a propagation mode cannot be established. This is the reason a band gap exists in photonic band structure. In the boundary condition concept, each of the waves needs to fulfill a boundary condition when multiple scattering occurs. However, in a certain frequency range, some of the waves cannot fulfill the boundary condition in periodic structure. This causes the existence of a band gap. Fundamental wave propagation can be categorized in two modes: the electric polarization (E polarization) mode and the magnetic polarization (H polarization) mode. A band gap that exists in only one of the modes is a partial band gap. If a band gap exists in both of the modes it is a complete band gap.

1.5 Left-Handed Metamaterials (LHMs) and Effective Plasma Frequency

Left-handed metamaterials (LHMs) are a new class of material that has been discussed by several investigators (Luo et al., 2002; Pendry, 1996; Pendry and Ramakrishna, 2003; Pendry et al., 1998; Pendry, 2000; Luo et al., 2003; Povinelli et al., 2003). The main characteristics of this type of material are a negative refractive index and negative permeability.

The existence of this type of material would change the concept of optical science because of the negative refractive index. It can help to overcome the

limitation of normal optical properties. The main application of LHMs is the superlens effect. This effect can help to overcome subwavelength focusing (Pendry, 2000). In the nature, all the materials possess only a positive refractive index. The smallest value of the refractive index for a known material in a vacuum is one. So, a question arises whether this class of materials really can exist. The first evidence for a negative refractive index was obtained by Shelby et al. (2001) using square copper split ring resonators and copper wire strips on fiberglass circuit board material. Then, Povinelli et al. (2003) and Luo et al. (2003) found that metallic photonic crystals can be used as LHMs. In this research, a series of photonic band structures for metallic photonic crystals using real materials was plotted. A negative slope is found in the photonic band structure if the material is LHM. The relationship for effective refractive index (Sakoda, 2005) in photonic crystals is

$$n_{eff} = \frac{a}{2L} \left(\frac{\Delta\omega a}{2\pi c} \right)^{-1} \quad (1.1)$$

where a is the lattice constant, L is the thickness, and $\frac{\Delta\omega a}{2\pi c}$ is the slope of the photonic band structure. Then, the relationship of effective permeability (Huang et al., 2004) is

$$\mu_{eff} = n_{eff} Z_{eff} \quad (1.2)$$

where $Z_{eff} = \frac{1+r}{1-r}$ and r is the complex reflectivity, which is smaller than one.

There is another property that has to be considered before a material is classified as an LHM is the effective plasma frequency. When the LHMs were first classified (Veselego, 1968), only negative refractive index (negative permeability)

cases were considered. More recently, Pendry (1996) found that photonic crystals that work as LHMs would couple with the low effective plasma frequency property. Effective plasma frequency and plasma frequency refer to two different physical parameters. Plasma frequency is used to describe the dielectric function of a bulk metal. This is well described in the Drude model (Nalwa, 2001):

$$\varepsilon(\omega) = 1 - \frac{\omega_p^2}{\omega(\omega - i\gamma)} \quad (1.3)$$

where ω_p is the plasma frequency and γ is the damping constant. But the effective plasma frequency $\nu_{p,eff}$ is the cutoff frequency of photonic crystal structures that involved a metallic component (Pendry, 1996). Metals are solid media and normally reflect the entire wave. But the Drude model predicts that when an electromagnetic wave is above a certain frequency, a metal is transparent and waves can penetrate through the metal. So, a low effective plasma frequency would make the metal transparent to waves at a lower frequency. Equations (1.4) through (1.7) are the analytical analysis of effective plasma frequency by several scientists.

Pendry, 1996; Pendry et al., 1998:

$$\nu_{p,eff}^2 = \frac{c^2}{2\pi a^2 \ln(a/r)} \quad (1.4)$$

Sarychev and Salaev (2001):

$$\nu_{p,eff}^2 = \frac{c^2}{2\pi a^2 [\ln(\sqrt{2} a/r) + \pi/2 - 3]} \quad (1.5)$$

Maslovski et al. (2002):

$$\nu_{p,eff}^2 = \frac{c^2}{2\pi a^2 \ln\left[\frac{a^2}{4r(a-r)}\right]} \quad (1.6)$$

Tretyakov (2004):

$$\nu_{p,eff}^2 = \frac{c^2}{2\pi a^2 [\ln(a/2\pi r) + 0.5275]} \quad (1.7)$$

where a is the lattice constant and r is the rod's radius. The effective plasma frequency is the minimum frequency for the first lowest band in a photonic band structure. For photonic crystals, which have extremely small filling fractions, the plasma frequency and effective plasma frequency should be the same. Researchers believe that the effective plasma frequency can be tailored by changing the arrangement of photonic crystals. Figure 1.4 shows the comparison of Equations (1.4) through (1.7).

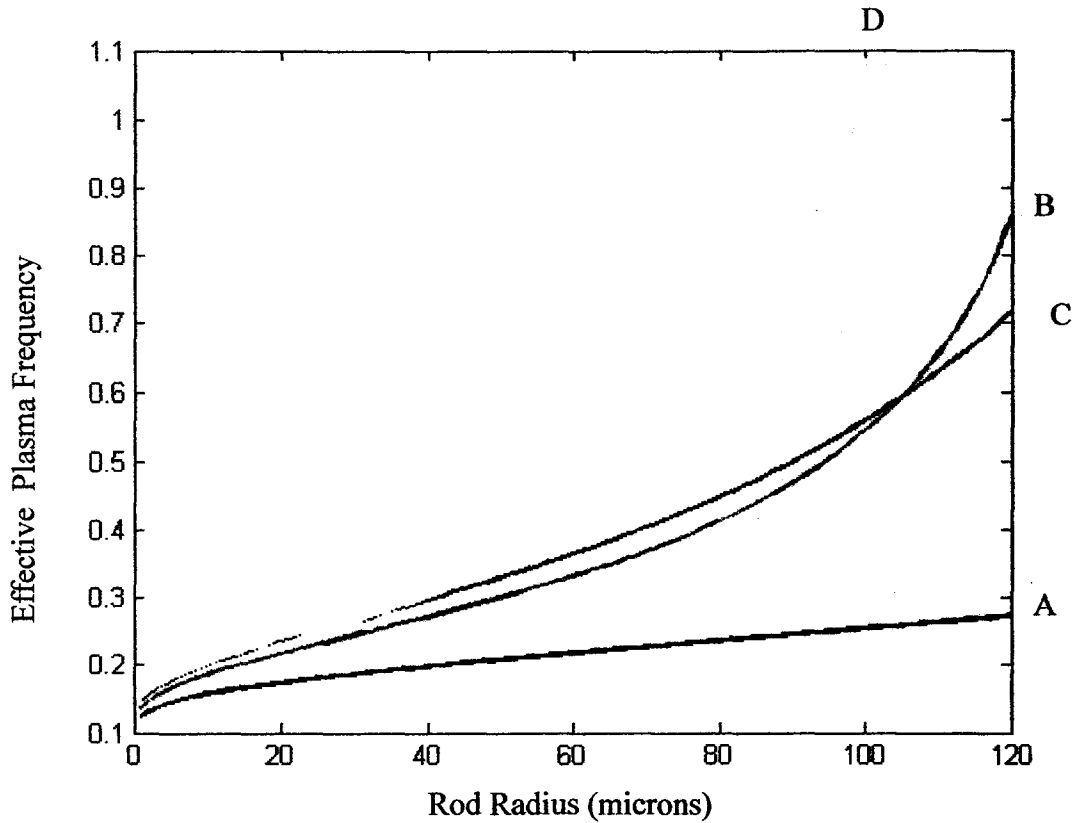


Figure 1.4: The effective plasma frequency as the function of rod radius using the expressions of (A) Pendry, 1996; Pendry et al., 1998, (B) Sarychev and Shalaev (2001), (C) Maslovski et al. (2002), and (D) Tretyakov (2004), where the lattice constant is 400 μm with copper rods in vacuum (Brand et al., 2007).

The analytical models for effective plasma frequency have been discussed. Brand et al. (2007) claimed the models are too simple to explain the effective plasma frequency for the photonic crystals with metal rods. The analytical model included only the lattice constant and size of rods of the structure. The effect of the dielectric constant used has not been discussed and related with the analytical model. So, in this thesis a new analytical model will be developed using numerical data for small dimensions photonic crystals. Then, by utilizing these plots, an investigation has been carried out to check whether this class of materials can really exist in this world.

1.6 Materials

In this research, several materials have been used to plot the photonic band structure. Some of the materials can create the photonic crystal effect. The investigation is needed because there still remain unknown properties of the materials suggested in this research that are used in photonic crystal structures. From photonic band structures, several properties can be investigated like band gap, negative refraction, strong curvature, group velocity anomaly, and slow light. These are the fundamental properties for scientists to use in understanding photonic crystals. The frequency-independent materials that are used in this research were selected according to the high dielectric contrast condition. This criterion has been discussed by Joannopoulos et al. (1997) and Xu et al. (2005) who said that the band gap appears at high dielectric contrast. Dielectric contrast is defined as the ratio of the dielectric constants of the high- ϵ and low- ϵ materials: $\epsilon_{high} / \epsilon_{low}$. But this fundamental rule is just a general idea from Joannopoulos et al. (1997). So, a series of investigations is needed.

The materials used in this research include teflon (polytetrafluoroethylene), a fluorocarbon solid material that has a low dielectric constant, $\epsilon_r = 2$ (James and Hall, 1989). It is widely used in high microwave frequency circuits. A flame-resistant 4 (FR-4) material which is a very common and widely used material in the electronic industry, made from the woven fiberglass cloth with an epoxy resin binder (Coombs, 2008). It has the dielectric constant $\epsilon_r = 4.9$. So, an investigation was needed to see whether this material has the potential to become photonic crystals when paired with other materials. Silicon dioxide (SiO_2), which has a dielectric constant $\epsilon_r = 3.2$, was also selected (Diebold, 2001). We also chose gallium arsenide (GaAs), which has a

dielectric constant $\epsilon_s = 12.96$ (Kasap and Capper, 2006). This creates a high dielectric contrast if paired with the low- ϵ materials. Finally, copper was selected as a frequency-dependent material. The plasma frequency ω_p of copper is 1914 THz or $\frac{\omega_p a}{2\pi c} \approx 1$ for a 1- μm lattice constant structure (El-Kady et al., 2000).

1.7 Simulation Software

Calculation software is needed to compile all the derived equations. Matlab was chosen for this purpose as our calculation involved complex and large matrices and Matlab is able to handle it very well. So, the photonic band structures in this thesis are plotted using Matlab. The commercial simulation software CST Microwave Studio (CST MWS) was also used. This software shows very high performance in investigating electromagnetic structures especially antennas, waveguides, and solar cells. The package is also able to calculate the structures not only at microwave wavelengths but also at optical wavelengths. It uses the finite difference time domain (FDTD) method as its calculation engine. This is a different calculation method than the PWE used in this research. So, it can be used to make a comparison with the results in this research. It also provides the scattering parameters of the electronic devices. Therefore this software is used to design the electronic devices as discussed in Chapter 8 and do some verification of photonic crystals. MEEP is free electromagnetic calculation software based on the finite difference time domain (FDTD), developed by a group of scientists from Massachusetts Institute of Technology led by Steven G. Johnson. This software is needed to verify some of the data for photonic crystals.

1.8 Objectives

In this research, there are several tasks which are left out in the literature and need to be studied. So, the objectives of the research can be summarized as below.

- 1) To investigate several properties of photonic crystals by using the plane wave expansion method.

In order to achieve the objective:

- i) A new equation is derived to calculate the photonic band structures of dielectric media containing metallic components.
 - ii) A new equation is derived for the photonic band structures of photonic crystals with dielectric rods in metallic media.
- 2) To derive a new analytical model using statistical analysis to explain the effective plasma frequency for both small dimensions photonic crystals containing metallic components and for small dimensions photonic crystals in metallic media.

1.9 Thesis Overview

Chapter 2 reviews the fundamental characteristics and basic calculations for photonic crystals. The calculations include the transformation of the reciprocal lattice in the Brillouin zone to be used in the plane wave expansion method. At the same time, the plane wave expansion method is reviewed. This method is used to investigate the photonic band structure of photonic crystals. Then, discussion on the effective plasma frequency of photonic crystals and plasma frequency of metallic materials is also presented.

In Chapter 3, some of the frequency-independent materials that are commonly used as photonic crystals are investigated. The photonic band structures are plotted with normalized frequency ($\frac{\omega a}{2\pi c}$) which lattice constant, $a = 1.0$ m and speed of light, $c = 3.0 \times 10^8$ ms⁻¹ to wave vector. The gap sizes of the materials are compared if the gap appears. So, the fundamental rule of photonic crystals, which is the relationship between the band gap existence and high dielectric contrast, is investigated.

In Chapters 4 and 5 we discuss the photonic crystals that consist of frequency-dependent materials. New equations for both E and H polarization are derived. A thorough discussion is presented on these different materials. These equations are used to calculate the photonic band structures of photonic crystals in dielectric media containing metallic components. Photonic band structures of different materials consisting of copper are discussed with normalized frequency ($\frac{\omega a}{2\pi c}$) with lattice constant, $a = 1.0$ μm and speed of light, $c = 3.0 \times 10^8$ ms⁻¹ to wave vector. Several properties of photonic crystals are obtained from the photonic band structure.

New photonic band structure equations for the photonic crystals that consist of dielectric rods in metallic media are presented in Chapters 6 and 7. These chapters discuss the photonic band structures of E and H polarization respectively. The focus is on the photonic band structures of photonic crystals that are made from different dielectric rods in copper media. The photonic band structures are plotted with normalized frequency ($\frac{\omega a}{2\pi c}$) with lattice constant, $a = 1.0$ μm and speed of light, $c =$

$3.0 \times 10^8 \text{ ms}^{-1}$ to wave vector. The optical properties of photonic crystals are derived from the photonic band structures.

The photonic band structures described in Chapters 4 through 7 are used to obtain the analytical model of effective plasma frequency of photonic crystals in the E polarization mode. Waveguides and microstrips constructed from photonic crystals are presented in Chapter 8. Conclusions and possible extensions to our work are discussed in Chapter 9.

Chapter 2

Photonic Crystals Theory and Methodology

2.1 Introduction

In this chapter the basic theory of photonic crystals will be introduced. The concepts of lattices and reciprocal lattices and the relation between periodic functions will be introduced as well as boundary conditions of different physical systems. Bloch's theorem and the Brillouin zone are also discussed. Then, the plane wave expansion method that is used for the frequency-independent material is also discussed.

2.2 Lattices and Reciprocal Lattices Theory

Photonic crystals are periodic dielectric structures. The lattices and reciprocal lattices theory are very important in understanding them. The reciprocal lattice is a very important concept in solid state physics because it helps us to obtain the band structures and understand the various properties of crystals (Khan, 2009).

We need to understand the translation of primitive vectors before we are able to understand the reciprocal lattice. To understand the translation vector, the 2-dimensional lattice concept is needed. The translation of vectors \mathbf{a}_1 , \mathbf{a}_2 , and \mathbf{a}_3 are implemented; they are not all in the same plane and are linearly independent. A 3D lattice consists of all points with position vector \mathbf{T} as shown below.

$$\mathbf{T} = n_1\mathbf{a}_1 + n_2\mathbf{a}_2 + n_3\mathbf{a}_3 \quad (2.1)$$

where n_1 and n_2 are integers. It can be used to present the lattice arrangement. The common arrangements in lattices are the square lattice and the triangular lattice. For reciprocal lattices, the definition will be

$$\mathbf{b}_1 = 2\pi \frac{\mathbf{a}_2 \times \mathbf{a}_3}{\mathbf{a}_1 \cdot \mathbf{a}_2 \times \mathbf{a}_3}; \mathbf{b}_2 = 2\pi \frac{\mathbf{a}_3 \times \mathbf{a}_1}{\mathbf{a}_1 \cdot \mathbf{a}_2 \times \mathbf{a}_3}; \mathbf{b}_3 = 2\pi \frac{\mathbf{a}_1 \times \mathbf{a}_2}{\mathbf{a}_1 \cdot \mathbf{a}_2 \times \mathbf{a}_3} \quad (2.2)$$

The points generated are

$$\mathbf{G} = h\mathbf{b}_1 + k\mathbf{b}_2 + l\mathbf{b}_3 \quad (2.3)$$

where h , k , and l are arbitrary integers that form the reciprocal lattice. So, for the case of 2-dimensional structures, the \mathbf{a}_3 and \mathbf{b}_3 will be ignored.

In the 2-dimensional periodic structure, the periodic function can be turned into

$$f(\mathbf{r} + \mathbf{a}_1) = f(\mathbf{r} + \mathbf{a}_2) = f(\mathbf{r}) \quad (2.4)$$

This means that each of the periodic functions is repeating the same process in the unit cell. We can change the $f(\mathbf{r})$ to a Fourier series because $f(\mathbf{r})$ is a repeating periodic function:

$$f(\mathbf{r}) = \sum_{\mathbf{G}} C(\mathbf{G}) \exp(i\mathbf{G} \cdot \mathbf{r}) \quad (2.5)$$

where \mathbf{G} is the reciprocal lattice that is defined in (2.3).

2.3 Bloch's Theorem

Bloch's Theorem is used for the study of wave propagation in a periodic system. This is a very important concept for the investigation of dielectric periodic systems. The

eigen states $\psi_k(r)$ of the one-electron Hamiltonian is $H = -\frac{\hbar^2}{2m} \nabla^2 + U(\mathbf{r})$ where

$U(\mathbf{r}+\mathbf{T}) = U(\mathbf{r})$ for all \mathbf{T} in a Bravais lattice (Khan, 2009). So, it can be chosen to

have the form of a plane wave times a function having the periodicity of the Bravais lattice:

$$\psi_{\mathbf{k}}(\mathbf{r}) = e^{i\mathbf{k}\cdot\mathbf{r}} u_{\mathbf{k}}(\mathbf{r}) \quad (2.6)$$

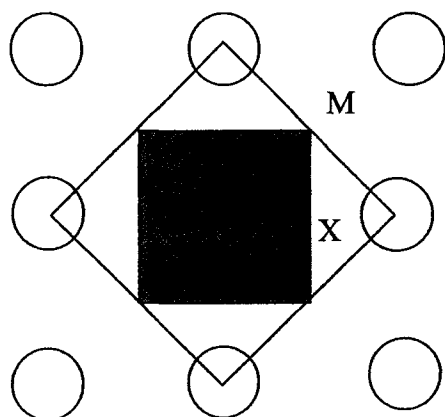
where

$$u_{\mathbf{k}}(\mathbf{r}+\mathbf{T}) = u_{\mathbf{k}}(\mathbf{r}) \quad (2.7)$$

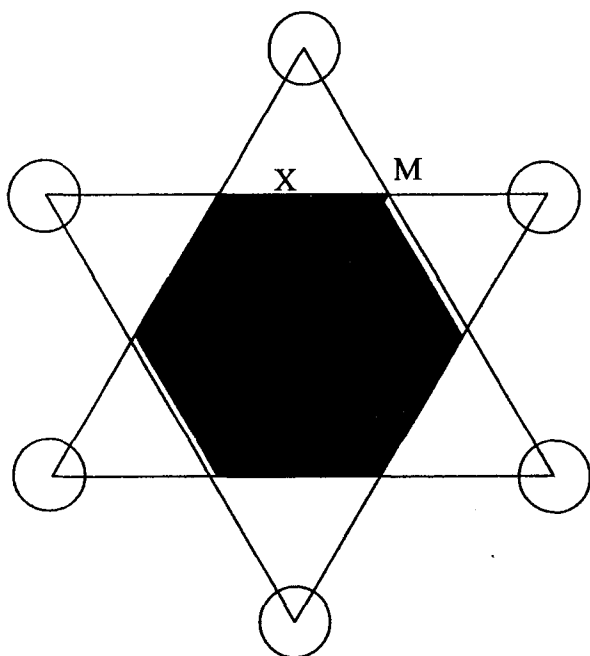
for all \mathbf{T} and $u_{\mathbf{k}}(\mathbf{r}) = \sum_{\mathbf{G}} u_{\mathbf{k}}(\mathbf{r}) \exp(i\mathbf{G}\cdot\mathbf{r})$ where \mathbf{k} is the wave vector and \mathbf{G} is the reciprocal lattice.

2.4 Filling Fraction and Brillouin Zone

The filling fraction f is a very important parameter in photonic crystals. In 2-dimensional systems, the filling fraction is defined as the percentage of cylinders that fill up a lattice. The maximum value of the filling fraction is one. The filling fraction is related to the rod size. So, each lattice arrangement has its own filling equation. The square and triangular lattice arrangement's filling fractions will be discussed in Sections 2.4.1 and 2.4.2 respectively. The Wigner-Seitz primitive cell of the reciprocal lattice is called the first Brillouin zone (Khan, 2009). The Brillouin zone is formed by joining other reciprocal lattice points to the origin followed by drawing perpendicular planes at the midpoint of these lines. We illustrate the definition in Figures 2.2(a) and (b) for square and triangular lattices respectively.



(a) Square Lattice



(b) Triangular Lattice

Figure 2.1: Irreducible Brillouin zones (red region) for (a) square lattice (b) triangular lattice.

2.4.1 Square Lattice

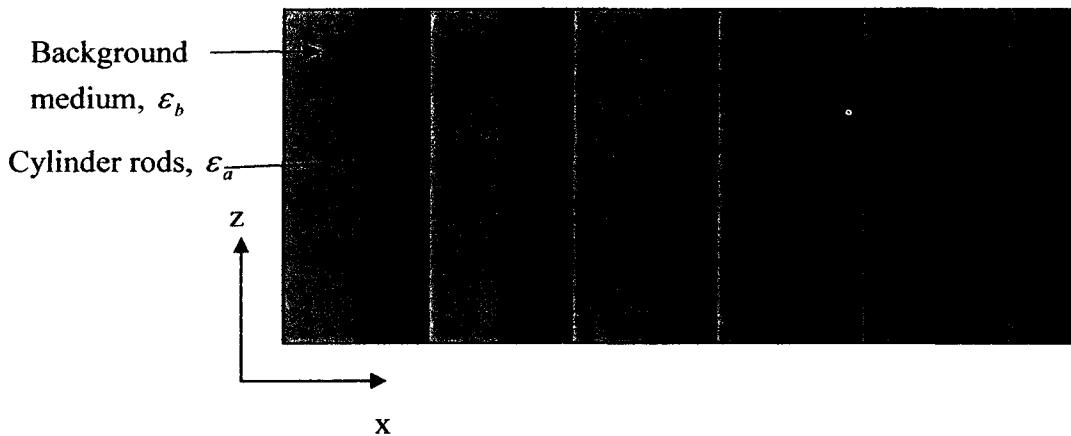
Equations (2.8) to (2.10) show the vector positions of the irreducible Brillouin zones for the square lattice.

$$\Gamma \rightarrow (k_x = 0, k_y = 0), \quad (2.8)$$

$$X \rightarrow \left(k_x = \frac{\pi}{a}, k_y = 0 \right), \quad (2.9)$$

$$M \rightarrow \left(k_x = \frac{\pi}{a}, k_y = \frac{\pi}{a} \right) \quad (2.10)$$

Calculation of the eigenfunctions is made in the first Brillouin zone of the photonic crystal structure. Two-dimensional square lattice photonic crystals are investigated. The arrangement is shown in Figure 2.2(a) and 2.2(b). It is the 2D crystal composed of a regular square array of circular dielectric cylinders.



(a)

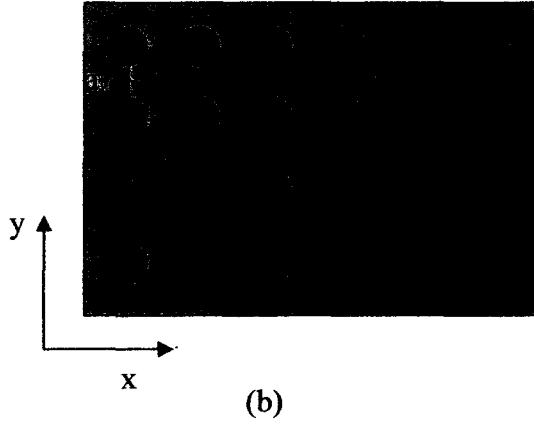


Figure 2.2: Photonic crystals of 2 dimensional square lattice in (a) cross-sectional view and (b) top view.

The lattice parameters a for the primitive translation vectors are

$$\mathbf{a}_1 = a(1, 0), \mathbf{a}_2 = a(0, 1) \quad (2.11)$$

while the vectors of the reciprocal lattice are

$$\mathbf{b}_1 = \frac{2\pi}{a}(1, 0), \mathbf{b}_2 = \frac{2\pi}{a}(0, 1) \quad (2.12)$$

The filling fraction of the square lattice is

$$f = \pi R^2 / a^2 \quad (2.13)$$

2.4.2 Triangular Lattice

Equations (2.14) to (2.16) show the vector position of the irreducible Brillouin zones of the triangular lattice.

$$\Gamma \rightarrow (k_x = 0, k_y = 0), \quad (2.14)$$

$$X \rightarrow \left(k_x = \frac{2\pi}{3a}, k_y = \frac{2\pi}{\sqrt{3}a} \right), \quad (2.15)$$

$$M \rightarrow \left(k_x = 0, k_y = \frac{2\pi}{\sqrt{3}a} \right) \quad (2.16)$$

where a is the lattice constant.

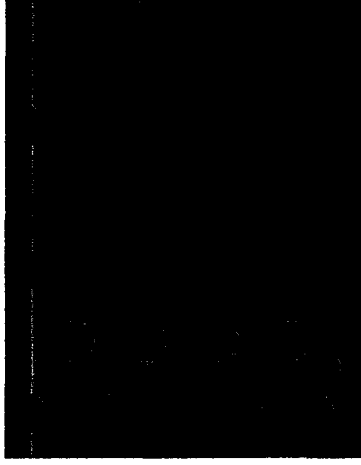


Figure 2.3: Top view of the 2-dimensional triangular lattice photonic crystals.

Figure 2.3 shows the arrangement of 2-dimensional crystals composed of an array of circular dielectric cylinders in a triangular lattice. So, we derived the reciprocal translation vectors as below. The primitive vectors are

$$\mathbf{a}_1 = a(1, 0), \mathbf{a}_2 = a\left(\frac{1}{2}, \frac{1}{2}\sqrt{3}\right) \quad (2.17)$$

then the reciprocal translation vectors are

$$\mathbf{b}_1 = \frac{2\pi}{a}\left(1, -\frac{1}{3}\sqrt{3}\right), \mathbf{b}_2 = \frac{2\pi}{a}\left(0, \frac{2}{3}\sqrt{3}\right) \quad (2.18)$$

The filling fraction of the triangular lattice is

$$f = (2\pi/\sqrt{3})R^2/a^2 \quad (2.19)$$

2.5 Plane Wave Expansion Method

In this section, the plane wave expansion method is reviewed. The band gap appears in photonic band structure of photonic crystals. The wave propagation will be inhibited in this area. So, to understand this band gap, the photonic band structure must be plotted. Then, from this photonic band structure, we learn the fundamental